BJES Basrah Journal for Engineering Sciences

Basrah Journal for Engineering Sciences, Vol. 21, No. 2, (2021), 12-16

Original Article

Journal homepage: www.bjes.edu.iq
ISSN (Online): 23118385, ISSN (Print): 18146120

OPEN ACCESS

Preparing Methane – Air Mixture Using Ejector

Tahseen Ali Jabbar [1,*], Masad Mezher Hasan [2], Safaa Hameed Faisal [3]

[1,2] Department of Fuel and Energy, Basrah Engineering Technical College, Southern Technical University, Basrah, Iraq
[3] Department of Thermal Mechanic, Basrah Engineering Technical College, Southern Technical University, Basrah, Iraq
E-mail addresses: tahseen.ali@stu.edu.iq , mesad.hassan@stu.edu.iq, s_hfaisal100@stu.edu.iq
Received: 2 January 2021; Revised: 4 March 2021; Accepted: 15 March 2021; Published: 11 July 2021

Abstract

In this research, a two – dimensional numerical investigation is conducted to show the ability of the jet-ejector to prepare the air – methane mixture at different equivalence ratio. The basic dimensions (diameters ratio, throat length, angle α, and angle θ) of the jet-ejector are taken into account on calculating the equivalence ratio. The results showed that the ratio of the diameters has a higher effect than other parameters on preparing a mixture for equivalent ratios including both rich and lean mixture. The rest of the factors did not have a significant effect on the value of the equivalence ratio, and only had a role in preparing an equivalence ratio for rich mixture type.

Keywords: Ejector, Equivalence Ratio, Air – Methane Mixture.

https://doi.org/10.33971/bjes.21.2.3

1. Introduction

An important part of the combustion process is to prepare a suitable mixture (fuel-air mixture). Several important elements depending on this mixture such as flame temperature and the number of pollutants. The arrangement of the fuel-air blend is, thusly, one of the most significant criteria for estimating the proficiency of ignition frameworks. Rahman et al. [1] contemplated the impact of the fuel-air proportion on the exhibition of the single-chamber hydrogen-powered port infusion motor. The model spoke to by one-dimensional gas elements stream and warmth move in the segments of the motor. The range investigation of the fuel-air proportion was from stoichiometry to lean. The outcomes show that the air-fuel proportion was significantly impacted by the presentation of hydrogen-powered motor particularly Brake Mean Effective Pressure (BMEP), warm proficiency and brake explicit fuel utilization (BSFC). Deng et al. [2] present a test study on the impact of the air-fuel proportion on the CO and NOx outflows in a bike motor fumes. The outcomes lit up that, the CO outflows strongly drop when the air-fuel blend changed from rich to lean. The NOx outflow at λ (overabundance air coefficient) and full motor burden is about 2.4 occasions of that at λ = 0.85. Hagos et al. [3] displayed exploratory aftereffects of the impact of air-fuel proportion on the burning qualities of a direct - infusion sparkle start motor fueled with a syngas of H/CO creation of equivalent molar proportion. The outcomes show that syngas worked under more extensive activity abundance air proportion (λ) when contrasted with CNG at a similar motor speed. Liu et al. [4] displayed the HC outflows trial estimations and consolidated reenactments on a twin-sparkle bike gas motor over a wide range condition. The outcomes lit up that, the general pattern of motor out HC sum diminishes as the relative air/fuel proportion increases. Leo [5] study the use of strategies dependent on the in-chamber pressure estimation that discovers far reaching applications. This paper centers around the identification of the Air-Fuel proportion and the in-chamber caught mass after the admission valve shutting from the in-chamber pressure signal. The Air-fuel proportion estimation may permit supplanting the lambda sensor, the estimation strategy depends on a measurable methodology. The outcomes show great exactness in anticipating Air-Fuel proportion and chamber caught mass in a wide motor working extent. Dahkil et al. [6] considered the impact of the essential weight and spout to the throat measurement proportion on the presentation of the air ejector. The outcomes show that higher weight proportion and the mass proportion (superior) happen when the spout to throat distance across proportion (DN/DT) was (5/8) and (1/8) individually.

2. Physical and numerical methodology

In this paper, CFD software (FLUENT) is used to simulate the flow field through the jet ejector. Steady-state 2D incompressible flow and the standard k-Є turbulent model are to solve the turbulent flow. Figure 1 shows the jet – ejector and the specifications of all the dimensions of this jet – ejector are shown in table 1. The Cartesian coordinate system was used to construct the problem. A CFD analysis of the entire domain of the geometry, it is necessary to set up the governing equations.

The governing equations could be solved with the aid of the following assumptions:

1. The flow is steady state.
2. The flow is turbulent and incompressible.
3. The ejector is at a horizontal plane.
4. The properties of flow are constant.
5. The body forces are neglected.
6. The effect of heat transfer is neglected.

The total kinetic energy before mixing is the sum of the kinetic energy between the motive and propelled stream. The kinetic energy of motive stream is [4]:

$$E = \frac{1}{2}\, mv^2 \tag{1}$$

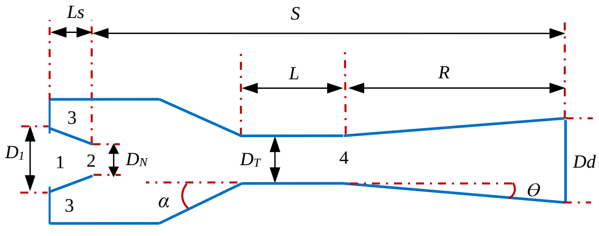

Fig. 1 the ejector geometry with the important dimensions.

And the continuity equations can be written as:

$$m_T = m_p + m_s \tag{2}$$

The equivalence ratio can be written as:

$$\Phi = \frac{\left(A/F\right)_{Stoich}}{\left(A/F\right)_{Act.}} \tag{3}$$

Table 1 the standard dimensions of jet – ejector using in this research [6].

Symbol	DT	S	D_1	R	L	L_s	DN/DT	θ	α
Value	6.98 mm	15DT	DT	12DT	4.5DT	2.25DT	1/2	5°	28°

The velocity of the mixture stream is computed by momentum conservation. Because of finite computational resources and the flow behavior in jet ejectors, the standard *k*-*ε* model is the best compared to other schemes, so the standard *k*-*ε* model is applied throughout the study.

Assuming that the fluid is compressible and viscous, the conservation equations of its mass, momentum, and energy can be written as [5]:

$$\frac{\partial}{\partial t}(\rho\varphi) + \frac{\partial}{\partial x}\left(\rho v_x \varphi - \Gamma_\varphi \frac{\partial \varphi}{\partial x}\right) + \frac{\partial}{\partial y}\left(\rho v_y \varphi - \Gamma_\varphi \frac{\partial \varphi}{\partial y}\right) + \frac{\partial}{\partial z}\left(\rho v_z \varphi - \Gamma_\varphi \frac{\partial \varphi}{\partial z}\right) = S_\varphi \tag{4}$$

Where: φ = dependent variable (velocity components, both kinetic and dissipation energies). Γ_φ = effective exchange variable coefficient of φ. S_φ = source term with the total pressure gradient. Eddy viscosity must be determined based on an adequate turbulent model. The standard *k*-*ε* model is a semi-empirical model for turbulent kinetic energy *k*, and its dissipation rate *ε*.

The turbulence kinetic energy *k*, and its dissipation rate ε, are calculated from:

$$\frac{Dk}{Dt} = \frac{\partial}{\partial X_i}\left\{\left\{(\nu\delta_{jk} + c_s \frac{k}{\varepsilon}\bar{u}_k\bar{u}_j)\frac{\partial k}{\partial X_k}\right\} - \bar{u}_k\bar{u}_j \frac{\partial u_i}{\partial X_k} - \varepsilon \right. \tag{5}$$

$$\frac{D\varepsilon}{Dt} = \frac{\partial}{\partial X_i}\left\{\left\{(\nu\delta_{jk} + c_1 \frac{k}{\varepsilon}\bar{u}_k\bar{u}_j)\frac{\partial \varepsilon}{\partial X_k}\right\} - \frac{\varepsilon}{k} c_2 \bar{u}_k\bar{u}_j \frac{\partial u_i}{\partial X_k} - c_3\varepsilon \right. \tag{6}$$

Model constants: *Cs*, C_1, C_2, and C_3 are 0.22, 0.18, 1.44, and 1.92 respectively [6].

2.2. Boundary conditions

2.2.1. Nozzle inlet

Flow at the nozzle inlet upstream of the step is considered to be isothermal, hydrodynamically steady and with distribution for the stream wise inlet pressure at values 1, 1.5, 2, 2.5, 3, 3.5, 4, 4.5, 5 and 5.5 bar.
Wall: no slip velocity

$$k_{in} = C_k\, w_{in}^2 \tag{7}$$

$$\varepsilon_{in} = C_\mu\, k_{in}^{3/2} / (0.5\, D_h C_\varepsilon) \tag{8}$$

Where C_k and C_ε are constants (C_k = 0.003, C_ε = 0.03) [8].
D_h: Hydraulic diameter

2.2.2. Outlet

The outlet pressure is zero. In addition, outflow condition and fully developed conditions at the diffuser exit.

$$\frac{\partial u}{\partial x} = \frac{\partial v}{\partial x} = \frac{\partial k}{\partial x} = \frac{\partial \varepsilon}{\partial x} = 0 \tag{9}$$

3. Results and Discussion

3.1. Mesh independent

To validate the results of this research, the mesh independent was be done. The equivalence ratio was adopted as a target function, and the effect of the mesh on the value of this function was calculated. Figure 2 shows the effect of the number of elements on the value of the equivalence ratio. It is possible to observe the stability of the value of the equivalence ratio when the number of elements become greater than 300000 elements. From this, that concluded it is possible to rely on the method of analyze.

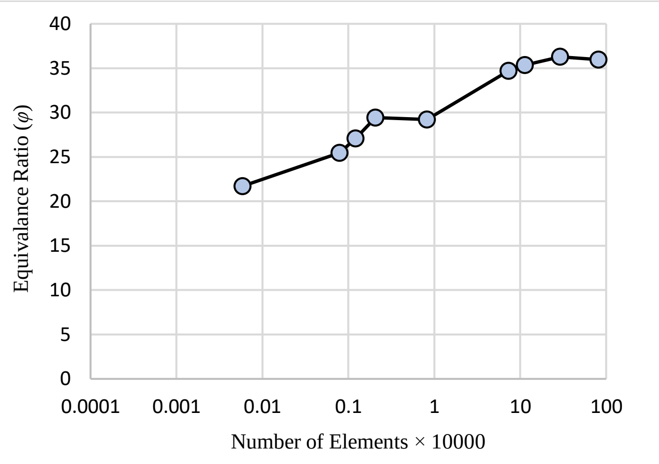

Fig. 2 Mesh dependent.

3.2. Pressure field

Figure 3 appears not to be the same throughout the study period. It shows the static pressure change in the inlet area of both air and methane with the diameter ratio. This figure can be divided into two parts, the first part (0 < y < 0.003 mm) is the main fluid entry area (air). The second part (0.003 mm < y < 0.007 mm) is the secondary fluid section area (methane). The first area is observed as the diameters ratio increases; the static pressure decreases due to decreasing flow resistance. Since the diameter of the ejector's throat is constant, then the increase in the ratio of diameters means an increase in the diameter of the nozzle. Because the flow is non-compressive (constant density), this causes a static pressure drop. This curve has a positive slope for the range (0.05 mm < DN/DT < 3.5 mm), while it has a negative slope for the range (3.5 mm < DN/DT < 4.5 mm). The explanation for this phenomenon is because the shape of the nozzle is the convergent nozzle for the first range, while it becomes a divergent nozzle for the second region. The second area of the curve (0.003 mm < y < 0.007 mm) is seen when the nozzle is convergent, the increase in the ratio of the diameters leads to a decrease in static pressure. However, if the nozzle is divergent, there is a relatively high in the static pressure when the ratio of the diameters increases. This difference in the performance of the nozzle leads to a decrease in the mass of air suction. In general, when increasing the ratio of the diameters leads to a decrease in the mass of air suction by the ejector.

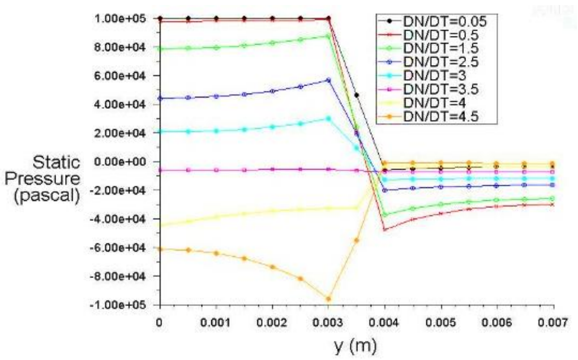

Fig. 3 the static pressure along both air and methane inlet region.

3.3. Diameters ratio

The effect of the ratio of the diameters on static pressure along the symmetry line can be illustrated in Fig. 4. The major event in this figure is that the mixing area (throat part) has a decrease in the static pressure with an increasing diameter ratio. This figure also shows static pressure change along with the nozzle ($0 < x < 0.01$ mm). Where the relationship is inverse, i.e., by increasing the diameter ratio, the static pressure along the nozzle will be decreased.

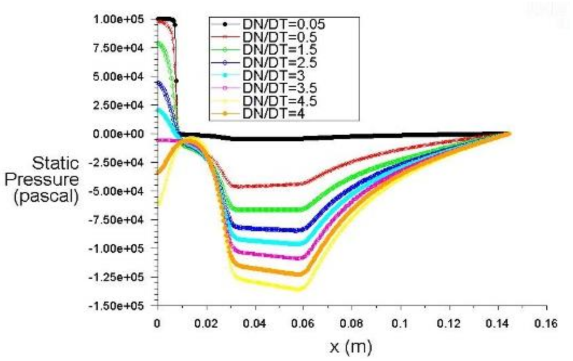

Fig. 4 the static pressure along the symmetry line of the ejector.

Figure 5 shows the relationship between the ratio of the diameters on the equivalence ratio at different primary pressures (1, 2, and 3 bar). Although, the initial pressure has changed, there is no significant effect on the equivalence ratio. This is important in using the ejector in preparing the equivalence ratio because it is not much affected by the initial pressure change. However, it is noted from this figure that the equivalence ratio is greatly affected by the ratio of the diameters. Besides, in this figure, there is a wide range of equivalence ratios, as the extent of the equivalence ratio $0 < \varphi < 64$. The increase of the ratio of the diameters causes the equivalence ratio to decrease due to the decrease in the suction mass of methane as illustrated in the discussion of Fig. 2.

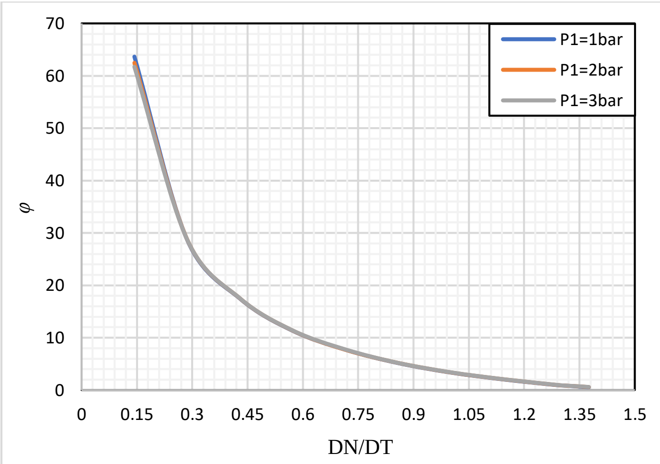

Fig. 5 The relationship between equivalence ratio and diameter ratio.

Figure 6 shows the effect of the diameters ratio on air mass (main fluid), methane mass (secondary fluid) and the mass ratio (methane to air ratio). Increasing the ratio of the diameters reduces the mass of methane while the air mass increases. Increasing the ratio of the diameters means increasing the area of the nozzle, which leads to an increase in the flow; it causes the air mass to increase. While the reduced in the suction mass of methane was attributed to reducing static pressure with increasing the ratio of the diameters in the suction area as illustrated in the discussion of Fig. 2. In Fig. 6, there is a certain optimization point where the values of the mass of air, methane, and the mass ratio are equally (equal to one) when the ratio of diameters is equal to 0.43.

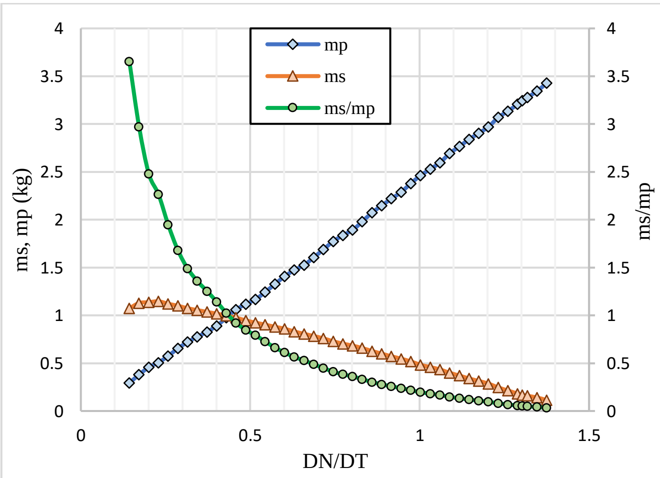

Fig. 6 the effect of the (DN/DT) ratio on ms, mp and ms/mp.

3.4. The throat length

Figure 7 shows the effect of the throat length (*L*) on the equivalence ratio, where the primary pressure was taken one bar. This figure is drawn within the boundaries of variable *L* (10 mm < L < 50 mm). The figure shows an inverse relationship between the throat length and the equivalence ratio, whereby increasing this length the equivalence ratio is reduced. Although the effect of the throat length on the equivalence ratio, its effect is not significant and within the limits of the fuel-rich mixture (16.9 < φ < 17.8).

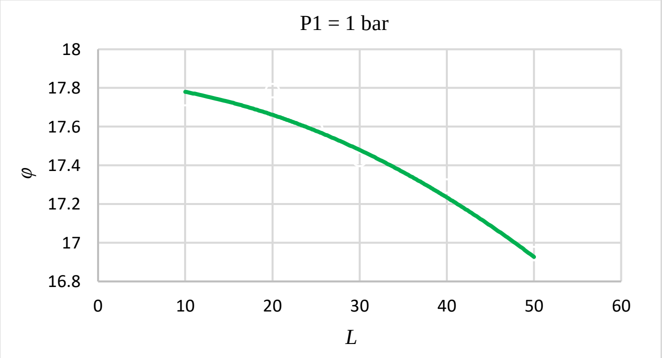

Fig. 7 the relationship between equivalence ratio and length (*L*).

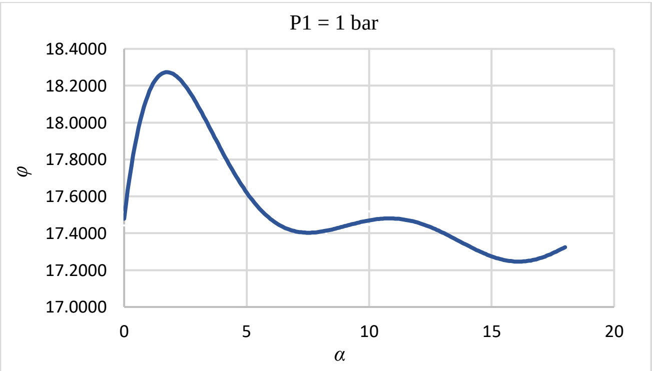

Fig. 8 the relationship between equivalence ratio and angle *α*.

3.5. The throat angle

The relationship between the throat entry angle and the equivalence ratio is shown in Fig. 8. From note this figure, it has no single performance along with the range of angle values (0 < *α* < 18°). The curve has a maximum equivalence ratio when the angle value is 9°, where the equivalence ratio is reached to 18.3. The most important observation on this figure is that the angle (*α*) effect is abbreviated to the rich mixture limits, i.e., a lean mixture cannot be produced depending on the change of this angle. This is important in the study of the performance of the ejector to products a Methane – air mixture, where there is no effect of the angle on changing the type of mixture (from a rich to a lean mixture or vice versa).

3.6. Diffuser angle

Figure 9 shows the relationship between the diffuser angle (*θ*) and the equivalence ratio. From the figure, we also note the effect of this angle only brief on the preparation of a rich mixture. Whereat the range of the study the equivalence ratio did not change its value of only slightly and within limits (10 to 20 rich conditions). This means there is no significant effect of the diffuser angle on the equivalence ratio. Therefore, it can make a future recommendation in the design of the ejector, the angle of the diffuser does not have a significant impact on the value of the equivalence ratio.

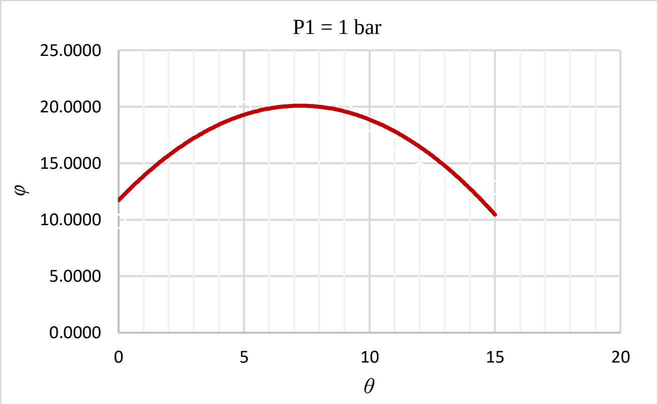

Fig. 9 the relationship between equivalence ratio and angle *θ*.

4. Conclusions

In this paper, two-dimensional numerical investigation is introduced to shows the ability of the ejector to preparing Methane – air mixture. The effects of diameters ratio on the air (mp), methane (ms) and mass ratio (ms/mp) were calculated using Fluent 16 code. The major conclusions were drawn as follows:

1. the increase of the diameter ratio leads to a decrease on the mass suction by ejector.
2. The initial pressure has no significant effect on the equivalence ratio.
3. Increasing diameters ratio resulted in decreasing in the equivalence ratio.
4. Throat length, angle *α*, and angle *θ* have no significant effects on the equivalence ratio. Also, it affects the equivalence ratio at the rich side only in a limited range propose in the current study.

Nomenclature	
Symbol	**Description**
D1	Nozzle inlet diameter
DN	Nozzle outlet diameter
DT	Throat diameter
Dd	Diffuser diameter
L	Throat length
L_s	Nozzle length
m_p	Primary mass flow rate
m_s	Secondary mass flow rate
m_T	Total mass
R	Diffuser Length
α	Inlet diffuser angle
θ	Outlet diffuser angle

References

[1] M. M. Rahman, M. K. Mohammed and Rosli A. Bakar, "Effects of Air-Fuel Ratio and Engine Speed on Performance of Hydrogen Fueled Port Injection Engine", Journal of Applied Sciences, Vol. 9, No. 6, pp. 1128-1134, 2009.

[2] B. Deng, Q. Li, Y. Chen, M. Li, A. Liu, J. Ran, Y. Xu, X. Liu, J. Fu and R. Feng, "The effect of air/fuel ratio on the CO and NOx emissions for a twin-spark motorcycle gasoline engine under wide range of operating conditions", Energy, Vol. 169, pp. 1202-1213, 2019.

[3] F. Y. Hagos, A. R. A. Aziz and S. A. Sulaiman, "Effect of Air-fuel Ratio on the Combustion Characteristics of Syngas (H_2 : CO) in Direct-injection Spark-ignition Engine", The 6th International Conference on Applied Energy - ICAE2014, Energy Procedia, Vol. 61, pp. 2567-2571, 2014.

[4] X. Liu, B. Deng, J. Fu, Z. Xu, J. Liu, M. Li, Q. Li, Z. Ma and R. Feng, "The effect of air/fuel composition on the HC emissions for a twin-spark motorcycle gasoline engine: A wide condition range study", Chemical Engineering Journal, Vol. 355, pp. 170-180, 2019.

[5] R. D. Leo, "Methodologies for Air-Fuel ratio and trapped mass estimation in Diesel engines using the in-cylinder pressure measurement", ATI 2015 – 70th Conference of the ATI Engineering Association, Energy Procedia, Vol. 82, pp. 957-964, 2015.

[6] S. F. Dahkil, T. A. Gabbar and D. K. Jaber, "Numerical Study of the Initial Pressure and Diameters Ratio Effect on The Jet Ejector Performance", Basrah Journal for Engineering Sciences, Vol. 14, No. l, 2014.

Biographies

Tahseen Ali Jabbar is a doctor of thermal Mechanical Engineering, Southern Technical University\Basrah Engineering Technical College. He received his Ph.D. in Mechanical Engineering from the Basrah University, Iraq. His research interests include Fluids, Heat Transfer, and Combustion.